Bandwidth Provision through Disjoint Multipath RPL in the IoMT

Souhila Kettouche[1], Moufida Maimour[2] and Lakhdar Derdouri[1]

[1]*RELA(CS)^2 labs, Larbi Ben M'hidi University, Oum El Bouaghi, Algeria*
[2]*Lorraine University, CNRS, CRAN, F-54000 Nancy, France*

Abstract

Internet of Multimedia Things (IoMT) is one extensively current topic of the Internet of Things (IoT) due to the immersive growth of multimedia applications in several fields. In LowPower and Lossy Networks (LLNs) where sensor nodes are a key component, providing a satisfactory quality of service (QoS) as well as a user quality of experience (QoE) for such applications is a challenging task. In fact, high bandwidth and substantial computation resources are required. To provide sufficient bandwidth to handle these high data rate applications, we propose to extend RPL to enable for simultaneous use of disjoint multiple paths. This is done on top of the already maintained DODAG structure with the least induced overhead. Furthermore, we suggest applying a low-complexity encoding method on the captured images. Based on both QoS and QoE metrics, we evaluate the performance of our disjoint multipath RPL (DM-RPL) for real video clip transmission using the IoT-LAB testbed. Our results show that multipath provides more bandwidth as the PDR is increased. Video quality is further improved thanks to the adopted data reduction at the source. All of this translates into less energy being consumed.

Keywords

Internet of Multimedia Things (IoMT), RPL, Multipath routing, Visual data transmission, Performance evaluation, QoE, QoS, Contiki OS, IoT-Lab

1. Introduction

The IoMT has undergone an unprecedented development these last years. This is confirmed by the massive use of multimedia applications in various fields such as smart homes and industrial monitoring. However, IoMT has stringent requirements compared to traditional IoT in terms of quality of service (QoS) as well as quality of experience (QoE). When it comes to handle multimedia applications characterised by their high data rate in wireless sensor networks (WSN), one of the basic building blocks of the IoT, the problem becomes more challenging because of their constrained resources. RPL [1] is the IETF standardised IPv6 Routing Protocol for low-power and lossy networks (LLNs) where directed-oriented acyclic graphs (DODAG) rooted at the sink are maintained. An objective function is used by each node to select its preferred parent toward the root node. Two objective functions namely, *ETX* [2] (default) and *OF0* (hops number) are predefined. Despite the fact that RPL almost meets the requirements of

LLNs to handle scalar data routing, it is still far from being able to allow real time streaming of video flows as it was mainly designed for low data traffic network [3]. To handle multimedia applications, some researchers proposed new objective functions based on energy [4, 5] or free bandwidth [6]. The proposed objective functions allow better behaviour when compared to predefined ones. However, the performance evaluation in both [4] and [6] does not consider real video traffic and the user QoE is not evaluated either. As for [5], simulations are based on H. 264 multimedia trace [7]. Nonetheless, H. 264 compression is not adapted to low-power video sensors [8]. Besides, the user QoE has not been assessed.

Multipath routing [9] has emerged in the last decades as a promising solution to provide sufficient bandwidth to handle high data rate flows. Extending RPL to allow for multipath routing has already been considered in the literature mainly to balance traffic among bottleneck nodes [10, 11, 12], improve data transmission reliability through replication [13] or mitigate congestion [14, 15]. The above multipath extensions are targeted to scalar data reporting and mostly make use of braided (non-disjoint) paths. More recently, authors of [16] leverage the RPL multi-instance opportunity to build multiple paths to enhance video delivery in the IoMT. A priority-based strategy is implemented where high priority frames are routed via the instance maintained using link quality as a metric and the low priority ones via the instance with the shortest path. They mainly showed by simulation that the disjoint multipath is more suitable to video delivery when compared to single and non-disjoint RPL variants.

Since a wireless network capacity is limited even with multipath routing, it still remains difficult to provide sufficient bandwidth able to satisfy the requirements of data intensive applications such as IoMT ones. Low complexity in-network data reduction is more than necessary to lower transmissions and the corresponding energy expenditure. Widely used standard video encoding techniques based on motion estimation algorithms such as MPEG-4, H.263 or H.264 are not suitable for sensor nodes [8].

In this paper, we aim to handle video delivery in the IoMT by addressing both facets of bandwidth scarcity problem. First, we propose a new algorithm to obtain disjoint multiple paths in RPL. Our extension do not leverage the multi-instance opportunity provided by RPL as in [16]. Instead, it uses existing RPL control messages to insure disjointness through the use of the IDs of the last hop nodes toward the DODAG root. Second, we make use of low-complexity video encoding more adapted to LLNs to reduce the amount of transmitted data. Our performance evaluation considers both QoS and QoE metrics and is carried on a real WSN testbed (IoT-LAB [17]). To the best of our knowledge, this is the first work that evaluates video transmission using multipath RPL on top of a real testbed with real video streams emulation. In this paper, we begin by presenting our disjoint multipath RPL (DM-RPL) protocol in Section 2. Afterwards, the compression method is presented in Section 3. The experimental scenario and the obtained results are discussed in Section 4 before concluding.

2. Disjoint Multipath RPL (DM-RPL)

The IoMT is made of a large number of small low-power devices that integrate sensors with on-board processing and wireless communication capabilities. Some of these devices ideally placed at strategic positions, are equipped by video cameras to provide richer and more informative

data on an area of interest. These sensor nodes are generally in charge of reporting information to a central gateway called the *Sink*. This delivery model is known as *convergecast* or multipoint to point communication. A WSN can be modelled as an unidirected connected graph $G(V, E)$ composed of a set of sensor nodes V and a set of links E. We consider the use of RPL to establish and maintain a DODAG structure rooted at the Sink $r \in V$ according to an appropriate objective function. This is achieved through the use of ICMPv6 packets called *DODAG Information Objects* (DIO). Based on the DODAG structure, each node v maintains a list of parents, one of which is designated as the preferred parent noted $\pi(v)$. A node willing to transmit data to the Sink, sends packets to its preferred parent. Let $T(V, E_T)$ be the spanning tree of G, rooted at the Sink (r), obtained by considering only links to preferred parents in the RPL DODAG rooted at r. We define the *depth d* of a node as the length (hops number) of its tree path to the root. The tree root has a depth $d(r) = 0$ and a non-root node $v \in T$ has a depth $d(v) = d(\pi(v)) + 1$. We call a *subtree* each tree rooted at a node $v \in T$ where $\pi(v) = r$ or equivalently $d(v) = 1$. The subtree rooted at v is noted T_v and v is designated as a *subroot*.

When dealing with high data rate applications, it is worth remembering the important limitations of LLNs. The available bandwidth is insufficient with respect to the requirements of these applications. In an attempt to provide additional bandwidth, we suggest to leverage simultaneous transmissions on multiple disjoint paths. To do so, we propose to extend RPL to allow for simultaneous use of multiple disjoint paths without incurring more overhead. The resulting protocol is called Disjoint Multipath RPL (DM-RPL). Paths disjointness from two nodes u and v to r using tree T child-parent links is guaranteed if these nodes belong to two different subtrees i.e. $u \in T_{t_u}$ and $v \in T_{t_v}$ with $t_u \neq t_v$. For a given source s, the default path is the one that follows the preferred parent at each hop. To get other paths that are disjoint, the source has to choose alternate parents that belong to different subtrees. In order to enable a node to identify the subtree to which belong each of its parents, one need to propagate the ID of each subroot downward. This is achieved by piggybacking this information in a field of DIO messages intended for this purpose we call PID (Path ID). It is initialised to zero in the initial DIO advertised by the DODAG root. Upon the reception of a DIO from the DODAG root, a subroot inserts its ID in the PID field before advertising the obtained DIO to its neighbours. When a regular node (other than root and subroots) receives a DIO message with non-zero PID field, it broadcasts it as it is. Based on the DIO information, a regular node updates its parents list as suggested by default RPL except that it records their PID. When the above process converges, each node in G will learn the ID of its subroot which is the last crossed node before last hop as well as the potential parents leading to the root via disjoint paths.

Figure 1 illustrates how DM-RPL maintains multiple disjoint paths based on the DODAG structure and the subroot ID propagation downward using DIO messages. The DODAG root r broadcasts a DIO message with a zeroed PID field. Each of the subroots i.e. nodes 1, 2 and 3, chooses r as its preferred parent and puts its own ID in the PID field before broadcasting the resulting DIO. Regular nodes (4, 5, 6 and 7), on the reception of a DIO, update the list of their parents. In each lower part of the circle representing a node, is given the list of the PIDs maintained where the first is the one related to the preferred parent. As depicted, node 4, for instance, has two disjoint paths via 1 and 2 respectively. For node 7, there are three possible paths highlighted in yellow for the primary one (via the preferred parent) and in green for the two alternative paths.
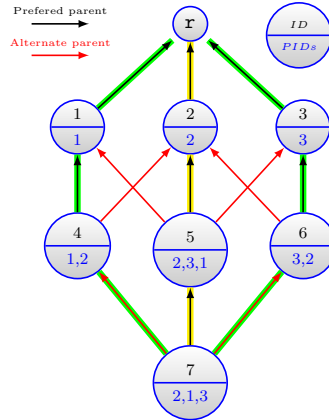
Figure 1: Illustrative example

3. Low Complexity Video Compression

Since an LLN network capacity is limited even when multiple paths are involved, it still remains difficult to provide sufficient bandwidth able to satisfy the requirements of data intensive applications such IoMT ones. Having sensors to deliver all the captured visual data is inefficient and has to be avoided. Authors of [18] showed that multipath routing allows to double the overall throughput. However, an acceptable video quality was difficult to obtain even when capturing and transmitting at only 6 fps a grey-scale low resolution video clip compressed using MPEG-4. As a result, in-network data reduction is more than necessary to lower transmissions and the corresponding energy expenditure. As already stated, MPEG-4 is not suitable for sensor nodes. Even JPEG low complexity still image compression algorithm is not very beneficial in terms of power consumption. This is mainly due to the discrete cosine transform (DCT) stage which consumes at least 60% of the whole power encoder [19, 20]. In order to suite the constrained nature of processing resources of low-power motes, we suggest to use a low complexity image compression provided by SenseVid [21], a video transmission and evaluation tool that considers LLNs specific characteristics.

A captured image is either intra-coded (M-frame) or inter-coded with respect to the previous M-frame in which case it is referred to as an S-frame. Whether a given frame is M- or S-encoded depends on the GOP coefficient (g). If $MSE \leq g^2$ where MSE is the mean square error with respect to the previous M-frame, then the frame is S-encoded ; otherwise, it is M-encoded. When $g = 0$ then all the frames are M-encoded. Increasing its value results in more S-frames and thus reduces the data rate. In what follows the process of encoding is detailed for each frame type.

3.1. Main Frame Encoding

Figure 2 shows the different steps of an M-frame encoding process. First, the image is decomposed into blocks of 8×8. Then, a fast pruned DCT called binDCT-C [22] is applied on each block with a triangular pattern [23]. Only coefficients located at the upper left triangle of side length $\rho \leq 8$ are considered. The resulting DCT block coefficients are quantised using the
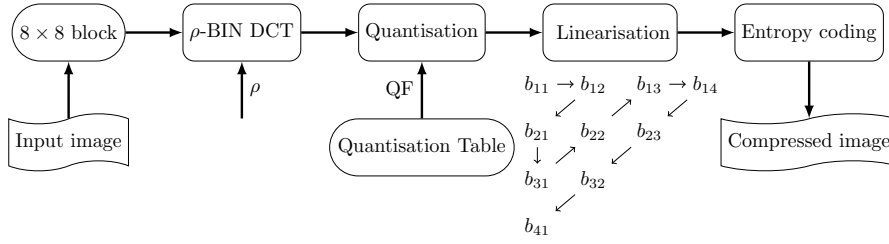
Figure 2: M-frame block encoding sequence ($\rho = 4$).
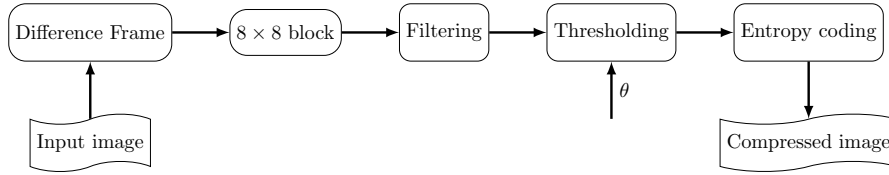

Figure 3: S-frame encoding sequence

JPEG standard quantisation matrix. Trade-off between quality level and compression rate can be obtained by selecting a proper quality factor (QF) that allows adjusting the quantisation matrix values. An image visual quality ranges from the poorest ($QF = 1$) to the best quality ($QF = 100$). The obtained block is then linearised following a zigzag scan before applying a lossless entropy encoding.

3.2. Secondary Frame Encoding

As shown in Figure 3, a secondary frame is inter-coded with respect to the previous main frame i.e. only blocks of the difference between the current frame and the previous M-frame are considered. To further save video sensors and network resources, a filtering and a threshold-ing operations are consecutively applied. Difference blocks with the least values that satisfy $\sum d_{ij}^2/64 \le 650$ are ignored. The retained blocks with difference values less than θ are zeroed. θ is the *threshold similarity* parameter provided by the user. Finally, a lossless entropy encoding is applied on the resulting non-null blocks. Note that since not all blocks are transmitted, blocks sequences have to be specified in the packet header. The sequence number of the first block of a packet is given as it is. A subsequent sequence is encoded using the difference with the respect to the previous one.

4. Experiment Results

Our experiments are made using IoT-LAB [17], a very large scale open experimental IoT testbed composed of 2728 static and mobile nodes distributed over six different sites in France (Strasbourg, Grenoble, Lille, Paris Saclay and Lyon). Three types of nodes, equipped with

(a) IoT-LAB interface with SenseVid.

(b) Tree Sample.
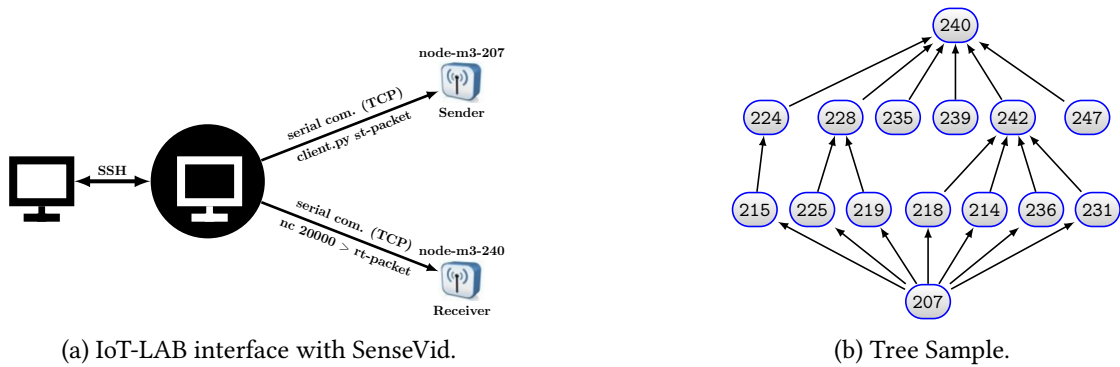
Figure 4: IoT-lab Experiment Setup

different micro-controllers and wireless communication chips, are provided namely, M3, A8 and WSN430 nodes. IoT-LAB can be accessed through a web portal or using provided command-line tools. Additionally, it offers a hosted environment on SSH front-ends with pre-installed command-line Tools and target architectures cross-compiler tool chains. It allows to retrieve experiments results and to access devices serial ports.

In order to assess the performances of our disjoint multipath routing, we extended the RPL implementation provided in the Contiki IPv6 network stack. The last two bytes of the IPv6 address of a node in IoT-LAB testbeds are used as an ID. Its uniqueness is ensured by the fact that only the last 16 bits are varied in the IPv6 address assignment and subnetting. In DM-RPL, this 16-bit ID is used to identify possible disjoint paths. The unused 7th (*Flags*) and 8th (*Reserved*) bytes of the DIO packet are chosen to constitute the PID field.

To carry out our experiments, we used M3 nodes installed in the F4 corridor of Grenoble site. Figure 4b shows the 15 used nodes and represents a possible tree structure in which the links are those connecting each node to its best parent. Since IoT-LAB does not provide video sensors, we emulate the transmission of a real video clip (by the node 207 to the root 240) using a traffic trace file (*st-packet*) generated by SenseVid. As shown by Figure 4a, a python script (*client.py*) gives transmission instructions to the source node. The RPL-UDP sender and receiver modules are modified to enable the former to send packets according to the instructions and the latter to retrieve the list of received packets to be stored in a receiver trace file (*rt-packet*). Based on this latter, SenseVid reconstructs the video received images and generates QoE video related metrics, namely, PSNR and SSIM [24].

We compare the performance of DM-RPL with default RPL and focus on the impact of increasing images frequency capture on their real time transmission. To do so and coping with LLNs constraints, we consider the transmission a given number ranging from 9 to 18 grey-scale images extracted from the original 300 ones of the hall monitor video clip [25]. Moreover, these images are down-sampled to a resolution of 128×128. We consider transmitting images encoded independently of each other (M-encoded) as well as the case of including some S-frames where the GOP coefficient g is set to 15 in order to reduce the data transmission rate as shown in Table 1. Used parameters are regrouped in Table 2. Each experiment is repeated at least 10 times to avoid fluctuation and obtained results are presented using box plots to show the

Table 1
Transmitted video characteristics

Images number	ref. PSNR (dB)		ref. SSIM		compression ratio (bpp)		transmission rate (Kbps)		packets to send		Frames sequence when $g = 15$
	$g = 0$	$g = 15$	$g = 0$	$g = 15$	$g = 0$	$g = 15$	$g = 0$	$g = 15$	$g = 0$	$g = 15$	
9	29.50	28.52	0.9081	0.8980	0.66	0.57	7.8	6.73	99	90	MMMMSMSMS
12	29.50	28.81	0.9010	0.8997	0.66	0.57	10.40	8.98	132	116	MMMMMSMMSMSM
15	29.50	28.05	0.9077	0.8959	0.66	0.52	13.01	10.32	165	140	MSMMMMSMSMSMSSM
18	29.51	28.31	0.9078	0.8960	0.66	0.51	15.6	11.94	198	162	MSMMMSMSSMSMSMSSMM

Table 2
Experimental Setup

Number of sensors	15 (m3, INRIA Grenoble)	Video duration	12 seconds
Packet max payload	128 Bytes	Frame resolution	128x128
Transport protocol	UDP	Quality Factor	5
Routing protocol	(IPv6) RPL, DM-RPL	Nb. captured images	9, 12, 15, 18
RPL objective function	ETX	GOP Coefficient (g)	0, 15
DIO max,min interval	17.5 min, 4 sec	DCT	Triangular BIN DCT
MAC	CSMA	DCT triangle side ρ	8
Radio Duty Cycling	ContikiMAC	Entropy coder	EG
Channel check rate	128 Hz		
reception sensitivity	101 dBm		
transmission power	0 dbm		

distribution of obtained values of the metric of concern. A segment and a small black square inside each rectangle shows the median and the mean values respectively.

Although, our multipath extension allows to build more paths, we conducted our experiments using only two paths. The obtained results and lessons learnt using two paths can be generalised to more paths and are expected for a future work. We first consider the packet delivery ratio (PDR) obtained by RPL (1-path) and DM-RPL (2-path) with the two sequences of frames ($g0$ and $g15$). As expected, Figure 5 shows a decreasing PDR when increasing the number of images to transmit due to a higher number of packets to transmit in a limited time window. Based on the mean PDR, DM-RPL outperforms RPL regardless of the transmission rate. DM-RPL is able to provide more bandwidth thanks to splitting the data flow on the two disjoint paths. Reducing the required bandwidth by inter-coding some of the frames ($g = 15$) allows to achieve better performances in terms of PDR when compared to the case where all frames are intra-coded ($g = 0$). This observation is valid for both RPL and DM-RPL.

Transmission rate reduction thanks to the introduction of S-frames leads to lower quality of images when compared to the use of only M-frames as shown by the obtained reference PSNR and SSIM given in Table 1. Hence, the quality of the received images has to be considered in the evaluation. Figure 6 shows both mean and distribution plots of the obtained PSNR and SSIM of the received images as reconstructed by SenseVid considering the incurred packet losses. Triangles in the candles curves depict the reference PSNR and SSIM. Once again, the quality is getting worse when increasing the transmission rate. The images quality is still fair
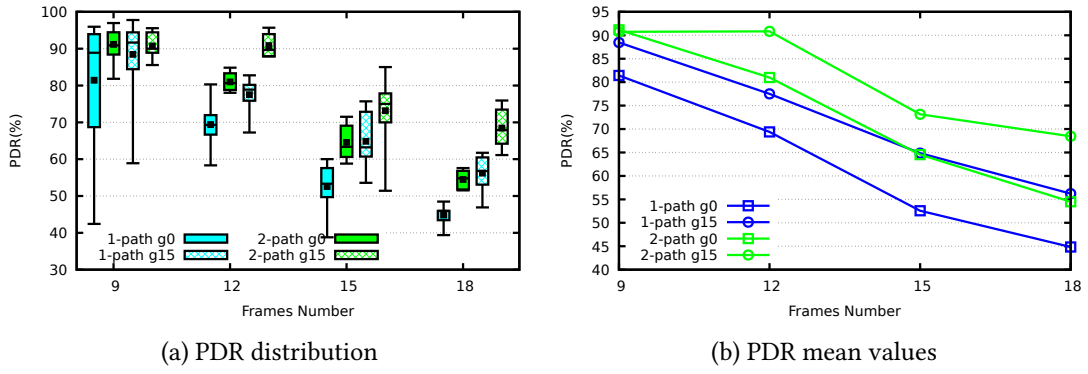
(a) PDR distribution

(b) PDR mean values

Figure 5: Packet Delivery Ratio

(a) PSNR distribution

(b) PSNR mean.

(c) SSIM distribution.
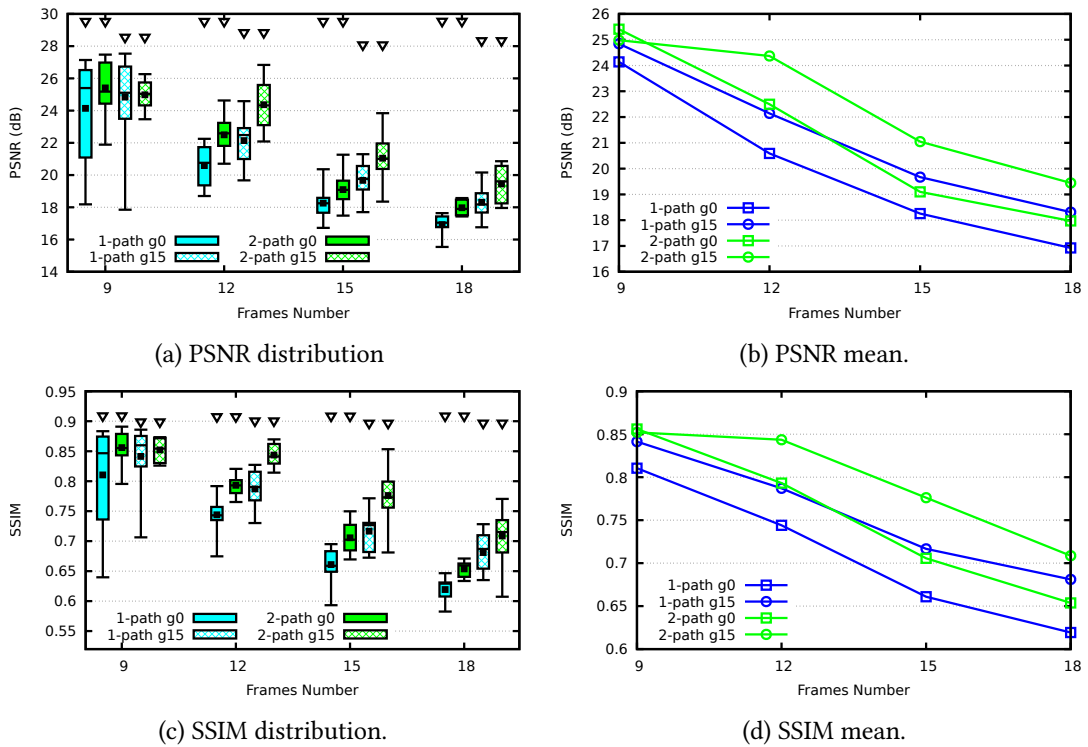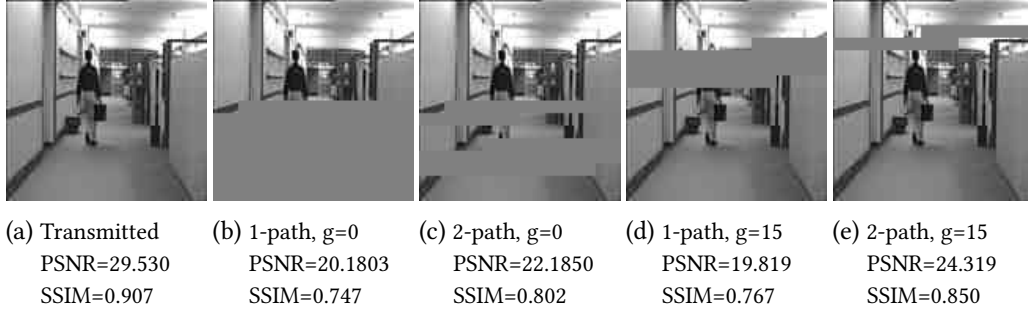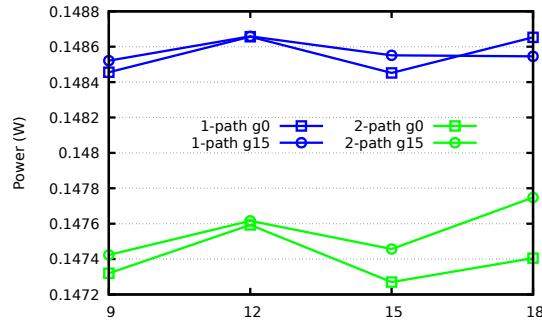

(d) SSIM mean.

Figure 6: Obtained Images Quality

($PSNR > 20$) for the evaluated schemes provided that the number of frames does not exceed 12. When using two paths along with more data reduction (2-path, $g15$), the quality remains acceptable even for the highest rate i.e. 18 frames captured and transmitted in real time. Note that the obtained PSNRs and SSIMs are higher when $g = 15$ compared to $g = 0$ even if the corresponding reference values are better in the latter case.

(a) Transmitted
PSNR=29.530
SSIM=0.907

(b) 1-path, g=0
PSNR=20.1803
SSIM=0.747

(c) 2-path, g=0
PSNR=22.1850
SSIM=0.802

(d) 1-path, g=15
PSNR=19.819
SSIM=0.767

(e) 2-path, g=15
PSNR=24.319
SSIM=0.850

Figure 7: Sample images for frame 3 when 12 frames are captured.

Figure 8: Mean Power Consumption

Figure 7 shows samples of the frame 3 when 12 images are captured and transmitted. The rightmost image is the one transmitted by the source. The others are those received by the Sink when using the four evaluated schemes. Data reduction strategy is profitable mainly when two paths are used where both PSNR and SSIM are improved.

Figure 8 plots the average consumed power for the different evaluated schemes when varying the number of captured frames. The results show that DM-RPL exhibits lower energy consumption compares to RPL. This is due to the fact that in DM-RPL, the traffic load is balanced on two paths. Thus, experimenting a lower number of packet losses which reduces the amount of MAC level retransmissions leading to lower energy expenditure.

5. Conclusion

In an attempt to handle multimedia traffic in constrained LLNs, we propose to extend RPL such that multiple disjoint paths can be maintained and used by video sensors. Moreover, we leverage low complexity compression techniques to cope with limited sensors resources. We carried out experiments using real WSN testbed and real video clip transmission. Both QoS (PDR and energy) and QoE (PSNR and SSIM) were adopted to assess the added value of our proposal. We mainly showed that using two paths allows to provide more bandwidth such that

the amount of successful transmissions is improved. Our used data reduction technique allows additionally for better images quality. Energy consumption is also improved.

Despite the obtained results, there is still a way to go to enhance the received images quality mainly when increasing the capture frequency. As a future work, we expect to improve our multipath strategy to obtain the best paths possible. Moreover, advanced encoding techniques with better optimised rate-distortion have to be investigated. Transmission strategies involving interleaving techniques are under study. Finally, advanced methods for image reconstruction with denoising and deblurring are to be explored.

Acknowledgments

References

[1] R. Alexander, A. Brandt, J. Vasseur, J. Hui, K. Pister, P. Thubert, P. Levis, R. Struik, R. Kelsey, T. Winter, RPL: IPv6 Routing Protocol for Low-Power and Lossy Networks, RFC 6550, 2012.

[2] D. S. J. De Couto, D. Aguayo, J. Bicket, R. Morris, A High-Throughput Path Metric for Multi-Hop Wireless Routing, in: Proceedings of the 9th ACM International Conference on Mobile Computing and Networking (MobiCom '03), San Diego, California, 2003.

[3] S. Kettouche, M. Maimour, L. Derdouri, QoE-based Performance Evaluation of Video Transmission using RPL in the IoMT, in: 2019 7th Mediterranean Congress of Telecommunications (CMT), ISSN null, 1–4, 2019.

[4] S. A. Alvi, G. A. Shah, W. Mahmood, Energy efficient green routing protocol for internet of multimedia things, in: 2015 IEEE Tenth International Conference on Intelligent Sensors, Sensor Networks and Information Processing (ISSNIP), IEEE, 1–6, 2015.

[5] F. Mortazavi, M. Khansari, An Energy-Aware RPL Routing Protocol for Internet of Multimedia Things, in: Proceedings of the International Conference on Smart Cities and Internet of Things, SCIOT '18, ACM, New York, NY, USA, ISBN 978-1-4503-6532-1, 11:1–11:6, 2018.

[6] H. Bouzebiba, M. Lehsaini, FreeBW-RPL: A New RPL Protocol Objective Function for Internet of Multimedia Things, Wireless Personal Communications (2020) 1–21.

[7] P. Seeling, M. Reisslein, B. Kulapala, Network performance evaluation using frame size and quality traces of single-layer and two-layer video: A tutorial, Communications Surveys Tutorials, IEEE 6 (3) (2004) 58–78, ISSN 1553-877X.

[8] B. A. B. Sarif, M. Pourazad, P. Nasiopoulos, V. C. M. Leung, A Study on the Power Consumption of H.264/AVC-Based Video Sensor Network, International Journal of Distributed Sensor Networks 11 (10) (2015) 304787.

[9] M. Maimour, Interference-aware multipath routing for WSNs: Overview and performance evaluation, Applied Computing and Informatics ISSN 2210-8327.

[10] O. Iova, F. Theoleyre, T. Noel, Exploiting multiple parents in RPL to improve both the net-

work lifetime and its stability, in: 2015 IEEE International Conference on Communications (ICC), IEEE, 610–616, 2015.

[11] M. N. Moghadam, H. Taheri, High throughput load balanced multipath routing in homogeneous wireless sensor networks, in: 2014 22nd Iranian Conference on Electrical Engineering (ICEE), IEEE, 1516–1521, 2014.

[12] L. Zhu, R. Wang, H. Yang, Multi-path data distribution mechanism based on rpl for energy consumption and time delay, Information 8 (4) (2017) 124.

[13] T. Lagos Jenschke, R.-A. Koutsiamanis, G. Z. Papadopoulos, N. Montavont, ODeSe: On-Demand Selection for multi-path RPL networks, Ad Hoc Networks 114, ISSN 15708705.

[14] M. A. Lodhi, A. Rehman, M. M. Khan, M. Asfand-e yar, F. B. Hussain, Transient Multipath routing protocol for low power and lossy networks., KSII Transactions on Internet & Information Systems 11 (4).

[15] Z. Wang, L. Zhang, Z. Zheng, J. Wang, Energy balancing RPL protocol with multipath for wireless sensor networks, Peer-to-Peer Networking and Applications 11 (5) (2018) 1085–1100.

[16] I. Bouacheria, Z. Bidai, B. Kechar, F. Sailhan, Leveraging Multi-Instance RPL Routing Protocol to Enhance the Video Traffic Delivery in IoMT, Wireless Personal Communications (2020) 1–30.

[17] C. Adjih, E. Baccelli, E. Fleury, G. Harter, N. Mitton, T. Noel, R. Pissard-Gibollet, F. Saint-Marcel, G. Schreiner, J. Vandaele, et al., FIT IoT-LAB: A large scale open experimental IoT testbed, in: 2015 IEEE 2nd World Forum on Internet of Things (WF-IoT), IEEE, 459–464, 2015.

[18] Z. Bidai, M. Maimour, Interference-aware Multipath Routing Protocol for Video Transmission over ZigBee Wireless Sensor Networks, in: IEEE (Ed.), the 4th International Conference on Multimedia Computing and Systems, IEEE, Marrakesh, Morocco, 2014.

[19] C. N. Taylor, D. Panigrahi, S. Dey, Design of an adaptive architecture for energy efficient wireless image communication, in: Embedded processor design challenges, Springer, 260–273, 2002.

[20] G. Suseela, Y. A. V. Phamila, Energy efficient image coding techniques for low power sensor nodes: A review, Ain Shams Engineering Journal 9 (4) (2018) 2961–2972.

[21] M. Maimour, SenseVid: A Traffic Trace based Tool for QoE Video Transmission Assessment Dedicated to Wireless Video Sensor Networks, Simulation Modelling Practice and Theory 87 (2018) 120–137.

[22] J. Liang, T. D. Tran, A Fast multiplierless approximations of the DCT with the lifting scheme, IEEE Transactions on Signal Processing 49 (2) (2001) 3032–3044.

[23] A. Mammeri, A. Khoumsi, D. Ziou, B. Hadjou, Modeling and Adapting JPEG to the Energy Requirements of VSN, in: Computer Communications and Networks, 2008. ICCCN '08. Proceedings of 17th International Conference on, ISSN 1095-2055, 1–6, 2008.

[24] M. Maimour, SenseVid: A traffic trace based tool for QoE Video transmission assessment dedicated to Wireless Video Sensor Networks, Simulation Modelling Practice and Theory 87 (2018) 120–137.

[25] YUV Video Sequences, URL http://trace.eas.asu.edu/yuv/index.html, ????